Lithium-Ion Batteries: Mussel-Inspired Adhesive Binders for High-Performance Silicon Nanoparticle Anodes in Lithium-Ion Batteries (Adv. Mater. 11/2013)

11 AUTHORS, INCLUDING:

Myung-Hyun Ryou
Hanbat National University
46 PUBLICATIONS **645** CITATIONS

SEE PROFILE

Jangbae Kim
Korea Advanced Institute of Science and Te…
27 PUBLICATIONS **762** CITATIONS

SEE PROFILE

Haeshin Lee
Korea Advanced Institute of Science and Te…
144 PUBLICATIONS **7,268** CITATIONS

SEE PROFILE

Jang Wook Choi
Korea Advanced Institute of Science and Te…
112 PUBLICATIONS **6,190** CITATIONS

SEE PROFILE

Mussel-Inspired Adhesive Binders for High-Performance Silicon Nanoparticle Anodes in Lithium-Ion Batteries

Myung-Hyun Ryou, Jangbae Kim, Inhwa Lee, Sunjin Kim, You Kyeong Jeong, Seonki Hong, Ji Hyun Ryu, Taek-Soo Kim, Jung-Ki Park,* Haeshin Lee,* and Jang Wook Choi*

Lithium-ion batteries (LIBs) are expanding their territory from conventional portable electronics to large-scale emerging applications, including various types of electric vehicles (EVs) and energy storage for utility grids.[1–5] In particular, the emergence of EVs is expected to solve critical issues relating to energy and the environment by causing a substantial decrease in the global dependence on petroleum and, at the same time, diminishing carbon dioxide emissions from vehicles.[3] In practice, however, the performance of current LIBs needs to be improved further with regard to energy density, cycle life, power capability, and safety before EV applications become a reality. Among these parameters, the energy density is a critical factor for EVs because it relates closely to acceptable driving distances upon a single refuel.

Recently, silicon has attracted considerable attention since it has potentially about 10 times the gravimetric capacity of conventional graphite anodes. The cycle lives of Si electrodes, however, are short, primarily as a result of their significant volume expansion by up to 300% upon full lithiation. Consequently, Si can become pulverized by the stress built up during the volume expansion. It has been found, however, that small-sized materials can relax the stress and can therefore overcome pulverization. The demonstration of enhanced cycle lives with various nanostructured Si electrodes[6–9] is reflective of this size effect. Although the pulverization issue is resolved by the use of nanometer-scale materials, the small size, in turn, weakens the interfacial contacts between Si and carbon conductors. Thus, the cycling performance is impaired quite severely. Also, the contact between the electrode film and current collectors can be loosened so that the electrode film can be peeled off during cycling with ease.[10–12] Thus, the role of binders is very critical for Si electrodes to maintain the electrode structure and thereby to achieve repeatable LIB operation.

Against this backdrop, we report in this Communication mussel-inspired binders (**Scheme 1**a) for high-performance Si nanoparticle (NP) anodes. Just as various motifs inspired by living organisms in nature have been utilized for practical applications,[13–16] mussels[4,5,17–19] have also provided creative motivations for exceptional adhesion properties even on wet surfaces (Scheme 1a). In particular, thorough investigations of mussel-inspired adhesive materials[16,18,20,21] have revealed that a certain functional group, namely catechol, plays a decisive role in the exceptional wetness-resistant adhesion.[16,21,22] In fact, the wetness-resistant adhesion could be very useful for battery operations because the battery components are also in contact with each other in liquid environments. Also, having taken note of the recent studies[11,12,23–25] that indicated the importance of the rigidity of polymer backbone in retaining the capacity of the Si electrodes during cycling, in the study reported here we conjugated adhesive catechol functional groups to well-known poly(acrylic acid) (PAA)[11,12,26,27] and alginate[11] backbones with high Young's moduli (Scheme 1b). As for the morphology of the active material, among various Si nanostructures, we chose Si NPs on account of their capability for mass production. The mussel-inspired binders endow Si NP electrodes (Scheme 1c) with markedly improved battery performance compared to those based on other existing binders.

Alginate (Alg) consists[28] of 1–4-linked β-D-mannuronic acid (M) and α-L-guluronic acid (G), which is structurally similar to carboxymethylcellulose (CMC), a binder widely used in silicon anodes. Alg acquires the mussel-inspired adhesive property by conjugation of dopamine hydrochloride to its carboxyl groups (Scheme 1b).[29] Materials and synthetic procedures are presented in the Supporting Information. Ultraviolet-visible (UV-vis) spectroscopic analyses verified that the dopamine is indeed conjugated to Alg and PAA, as indicated (**Figure 1**a) by the presence of a peak at 280 nm. The absorbance at 280 nm was used to quantify the extent of catechol conjugation onto the carboxylic acid groups of Alg and PAA. By comparative characterization

Dr. M.-H. Ryou, Prof. J.-K. Park
Graduate School of EEWS (WCU) and Department
of Chemical and Biomolecular Engineering
Korea Advanced Institute of Science and Technology
Daejeon, 305-701, Republic of Korea
E-mail: jungpark@kaist.ac.kr

Dr. J. Kim, S. Kim, S. Hong, J. H. Ryu, Prof. H. Lee
Department of Chemistry
Graduate School of Nanoscience and Technology (WCU)
and KAIST Institute NanoCentury
Korea Advanced Institute of Science and Technology
Daejeon, 305-701, Republic of Korea
E-mail: haeshin@kaist.ac.kr

I. Lee, Prof. T.-S. Kim
Department of Mechanical Engineering and
KAIST Institute Eco-Energy
Korea Advanced Institute of Science and Technology
Daejeon, 305-701, Republic of Korea

Y. K. Jeong, Prof. J. W. Choi
Graduate School of EEWS (WCU) and KAIST Institute NanoCentury
Korea Advanced Institute of Science and Technology
Daejeon, 305-701, Korea
E-mail: jangwookchoi@kaist.ac.kr
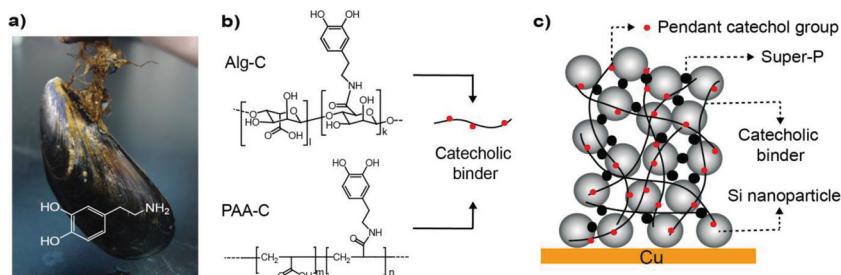
Scheme 1. Catechol conjugated polymer binders and Si anode structure. a) Mussel; the inset shows the chemical structure of dopamine inspired from mussel foot proteins. b) Structural formula of Alg-C and PAA-C alongside a simplified structure of a conjugated polymer binder; the black solid line represents the polymer backbone with carboxylic acid functional groups attached and red circles represent catechol moieties conjugated to the backbone. c) A graphical illustration of the Si NP anode structure.

with dopamine solutions of standard concentrations, we found that (3.4% ± 0.4%) and (2.8% ± 0.2%) of the carboxylic acid groups of Alg and PAA, respectively, were conjugated with dopamine. Furthermore, X-ray photoelectron spectroscopy (XPS) confirmed the dopamine conjugation, since the nitrogen 1s peak originating from amide bonds (Scheme 1b) appeared

around 399 eV (Figure 1b and Figure S1 in the Supporting Information). By contrast, no noticeable N 1s peak was detected in unmodified Alg (Figure 1b) and PAA (Supporting Information, Figure S1).

As an effort to quantitatively examine the binder–Si interactions in single-molecular resolution, atomic force microscopy (AFM) pulling tests were conducted. For the mussel-inspired adhesive binders, Alg-C was tested as a representative case and was compared against control cases of Alg and poly(vinylidene fluoride) (PVDF). The mussel-inspired adhesive catechols in Alg-C exhibit significantly enhanced interactions with silicon surfaces. Silicon nitride cantilevers with a spring constant of ~250 pN nm^{-1} were dipped into the solutions of either Alg-C or Alg (0.5 mg mL^{-1}). After the binder-adsorbed cantilevers had been rinsed with excess double-distilled water (DDW), the cantilevers were integrated into an atomic force microscope and the binder–Si interactions were measured (Figure 1c). See the Supporting Information for experimental details. Catechol–Si interaction forces
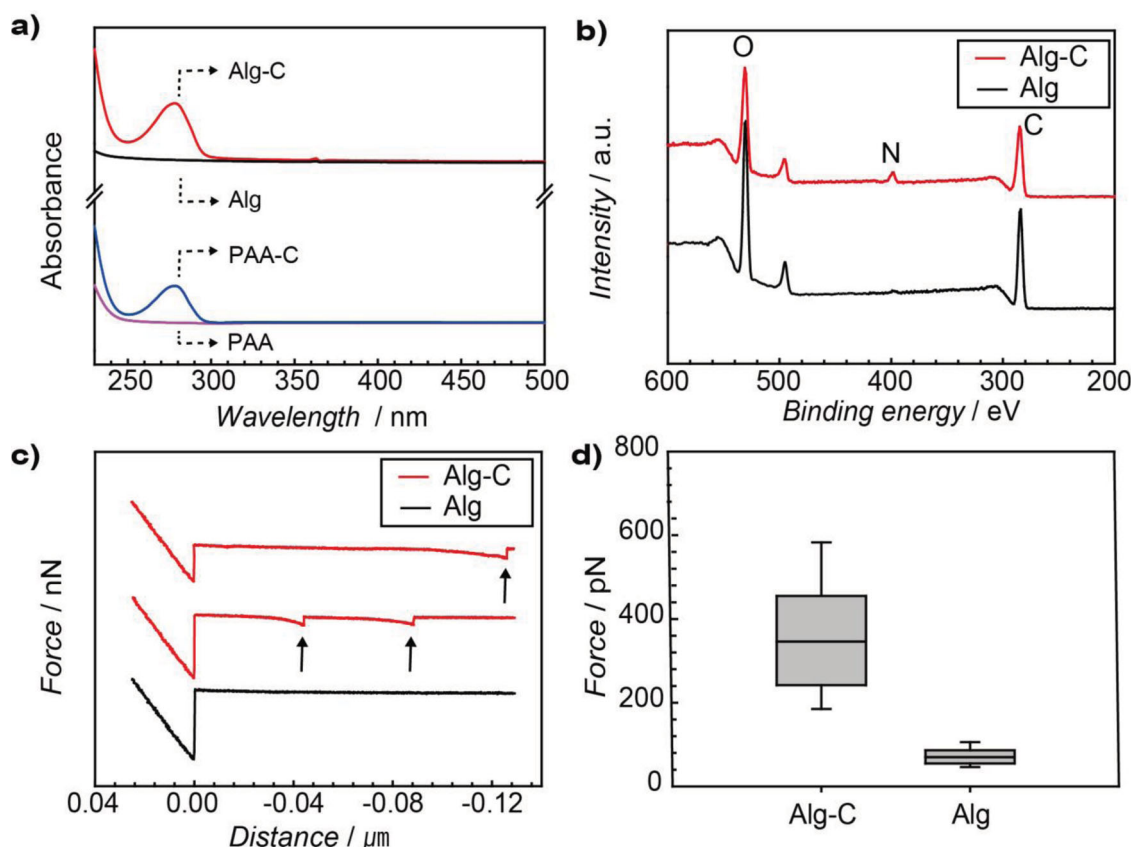

Figure 1. Characterization of Alg, Alg-C, PAA, and PAA-C. a) UV-vis spectra of polymer binders. The UV-vis spectra of Alg-C and PAA-C show characteristic absorption peaks at 280 nm commensurate with catechol conjugation. b) XPS spectra of polymer binders. The XPS spectrum of Alg-C (red) reveals the N 1s peak, indicating the existence of dopamine moieties. c) Force–distance (F–D) curves of Alg-C and Alg obtained by AFM experiments. The two representative F–D curves of Alg-C indicate the catecholic interaction between the Si surface and cantilever during the lifting procedure. d) Measured interaction forces of Alg-C (n = 272) and Alg (n = 52) from the AFM experiments in (c).

Materials
Views
www.MaterialsViews.com

ADVANCED
MATERIALS
www.advmat.de

COMMUNICATION

at a single-molecule level were conspicuously observed for Alg-C (arrows, red spectra), whereas no noticeably large force was detected for Alg (black spectrum). The double detachments indicate that multiple catechols are conjugated to the alginate backbone (middle, red). The averaged force values are 370 pN (n = 272) for Alg-C and 73 pN for Alg (n = 52) (Figure 1d). The observed force magnitude (catechol–Si) is smaller than that reported[21] for single-molecule interaction between catechol and Ti (~750 pN). While the observed catechol–Si interaction falls in the force range of coordination bonds, which is typically[30] several hundred piconewtons, further investigation is necessary to explain the decrease in the catechol–Si interaction compared with the catechol–Ti one. The interactions between Alg and Si (~73 pN) might be primarily a result of hydrogen bonding, which usually[31] has a force value less than 100 pN.

Consistent with the results at the single-molecule scale, the superior adhesive properties of Alg-C (compared to Alg and PVDF) were observed in experiments involving bulk-scale peeling mechanics (**Figure 2**). This peeling test has been widely adopted[10,32,33] to evaluate the adhesion of diverse binders to Si anodes, and detailed procedures are presented in the Supporting Information. The initial peeling force increases by about 100% when the binder changes from Alg to Alg-C: ~0.3 N for Alg and ~0.6 N for Alg-C. Note the first arrow in Figure 2a. Also, the sharp and discrete peaks indicated by the arrows were frequently detected in the force–displacement curve of the Si electrodes with Alg-C (Si-Alg-C). By contrast, this characteristic was not observed in the Si electrodes with Alg (Si-Alg) and PVDF (Si-PVDF). The sharp peaks in the Si-Alg-C data can be well resolved in the enlarged force–displacement curve (Figure 2b). This observation may be interpreted in terms of a number of catechol groups becoming collectively detached from the silicon surface. Moreover, the enhanced adhesion of Si-Alg-C was visualized by the presence of the crack tip (Figure 2c). The binders can be directly observed at the peeling interface between the detached electrode film and Cu foils. At this interface, Si-Alg-C shows much more elongated bridges than those observed for Si-Alg and Si-PVDF, indicating much better film adhesion caused by Alg-C. While the oxidation states of catechols surely play a role in the adhesion, analysis of the oxidation states of catechols in the present polymer binders is difficult because of the low degree of conjugation. Nonetheless, the catechol moieties conjugated to the polymer binders might not be completely oxidized.[34–36] This is partly because the catechols participating in binding to the surface-exposed atoms (Si in the current case) might result in the prevention of electron movement or other types of electron transition.

Coin-type half-cells that employ Li metal as both the reference and counter electrodes were tested by galvanostatic measurements in order to investigate the effect of the mussel-inspired binders on the electrochemical performance of Si NP cells. Lithium hexafluorophosphate (1 M $LiPF_6$) was dissolved in the co-solvent ethylene carbonate (EC) and diethyl carbonate (DEC) (1:1 by weight) for an electrolyte. Tests consist typically of precycling at C/10 rate and subsequent actual cycling at various rates higher than C/10. It is noteworthy that attaining good cell performance from the electrode fabricated with Si NPs is a more challenging task than the cases of other Si nanostructures. Si
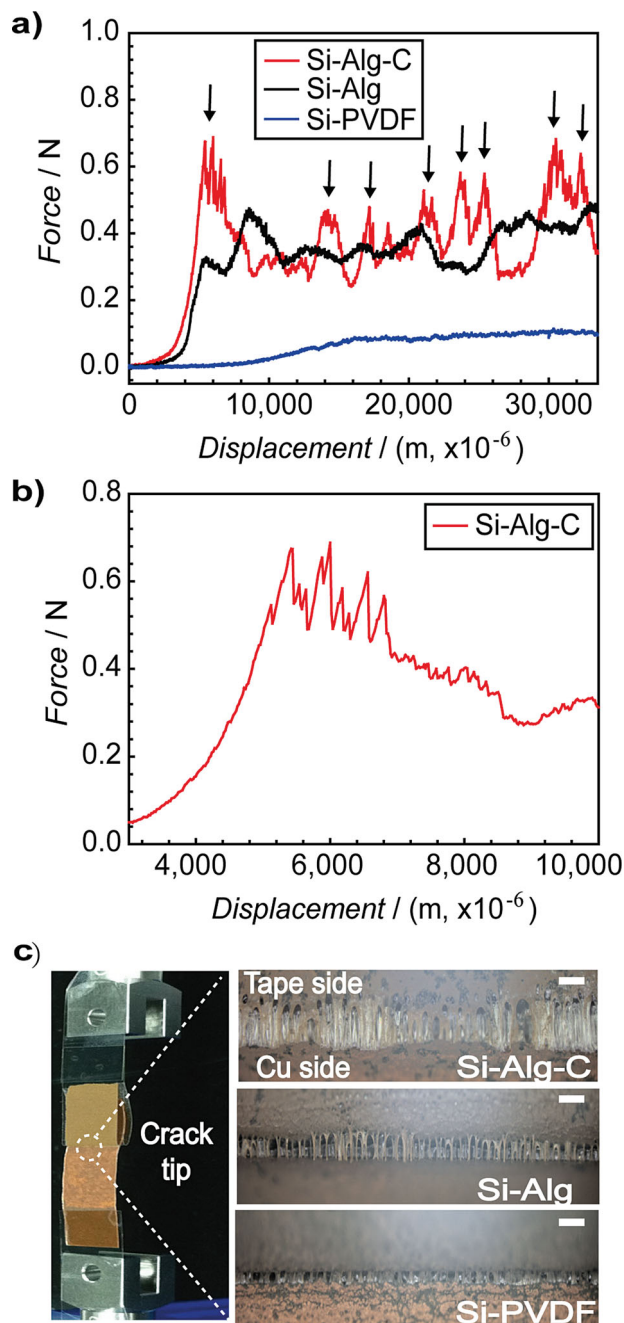
Figure 2. Peeling tests for the Si NP electrodes with various binders. a) Force–distance (F–D) curves of the Si electrodes with Alg-C, Alg, and PVDF. b) Enlarged F–D curve for Si-Alg-C, which corresponds to the first peak region indicated by the first arrow in (a). c) Left: A photograph of the peeling test setup. Right: Optical microscopy images at the crack tips where electrode films attached to 3M tapes are pulled from Cu foils. Binder bridges at the crack tips are clearly seen. The scale bars represent 200 μm.

NP cells usually show lower specific capacities and poor capacity retention over cycling, mostly because of the weak interfacial contacts between Si NPs and carbon conductors, caused by the volume change of Si.[10,37] In an effort to overcome the unstable

contacts, various binders have been tested,[11,12,23,25,32,38] and it transpires that Alg[11] and PAA[12] outperform other binders, such as CMC and PVDF, with Si NP electrodes. The superior performance of the Alg and PAA binders was ascribed to the stiff nature of their backbone, as well as to the presence of carboxylic acid groups, which form hydrogen bonds (H-bonds) with the silicon oxide surfaces of Si NPs.[11,12] For reasonable cell performance, however, these binders still require unrealistically excessive amounts of binders and carbon conductors[12] or limited mass loadings of Si active materials.[11]

In galvanostatic measurements (**Figure 3**a) with the potential range of 0.01–1.0 V (versus Li/Li+), charge–discharge takes place around 0.15 and 0.4 V, respectively, which is consistent with previously reported values for other Si anodes.[6] Importantly, the Si NP cells with different binders show remarkably different specific capacities in the precycling. Si-Alg-C, Si-Alg, Si electrodes with PAA-C (Si-PAA-C), Si electrodes with PAA (Si-PAA), and Si-PVDF exhibit reversible capacities of 3440, 3250, 3500, 3180, and 1966 mAh g^{-1}, respectively, with Coulombic efficiencies of 60.1, 60.1, 71.2, 72.3, and 63.1% (Supporting Information, Figure S2) Obviously, Si-Alg-C and Si-PAA-C show higher

capacities than their counterparts without catechol groups, verifying the importance of catechol groups in preserving the contacts between Si NPs and carbon conductors. In the case of the catechol-conjugated binders, the robust contacts promote efficient electrical conducting pathways within the electrodes and, as a result, the portion of dead Si is decreased. The capacity trend was also confirmed by cyclic voltammetry (CV) measurements (Supporting Information, Figure S3). In addition, control tests that examined the capacities of the binders alone, for both cases with and without the conductive carbon black Super P in the electrode films, confirm that the binders themselves do not display tangible capacities as active materials (Supporting Information, Figure S4–S6) because electrochemical activity of catechols has been detected in the potentials beyond the operating potentials of Si anodes.[39,40] From these experiments, it can be concluded that Alg-C itself makes no contribution to the increased capacity of Si-Alg-C.

The different capacities result from distinct adhesive properties of the binders: PVDF is known[12] to bind with the silicon oxide surface based on weak van der Waals interaction. On the other hand, Alg and PAA are known to form H-bonds between
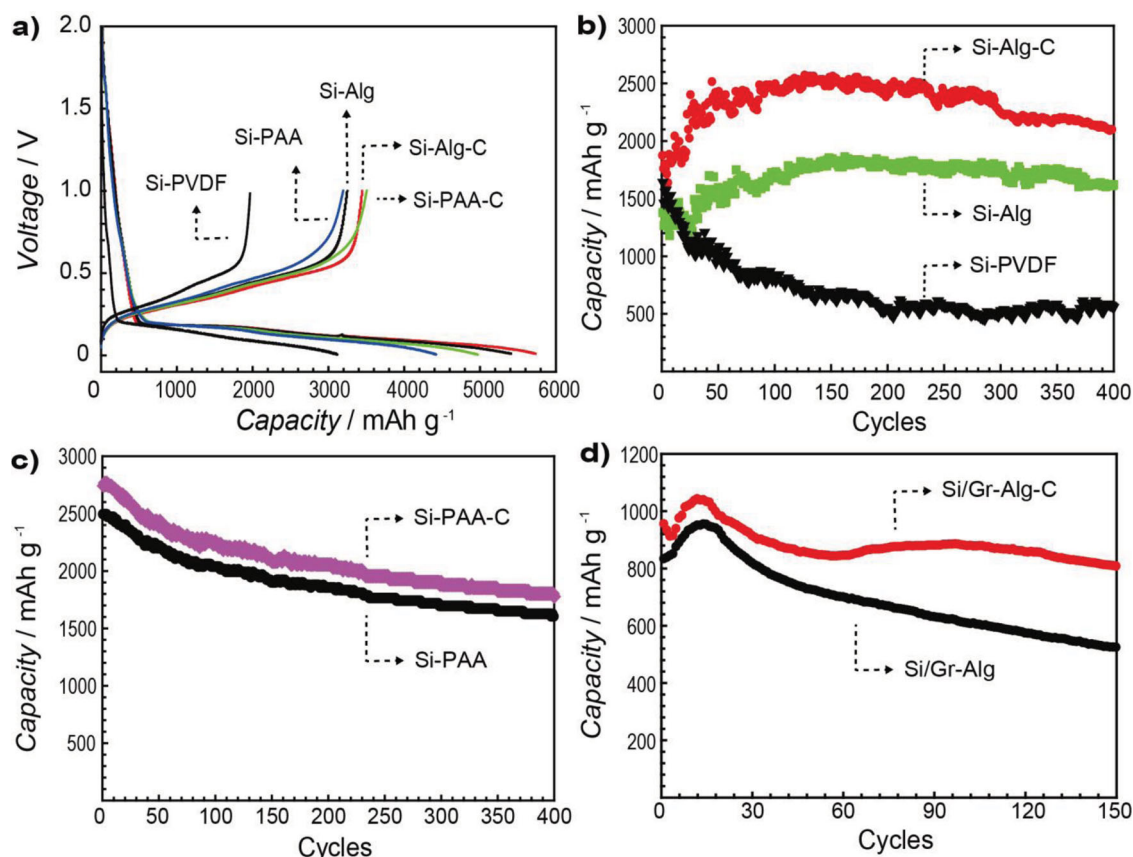
Figure 3. a) Potential profiles of the cells with various binders during the precycling. The cells were measured at C/10 rate (420 mA g^{-1}) in the range of 0.01–1.0 V (versus Li/Li+). b) The cycling performance of the Si electrodes based on the Alg-C, Alg and PVDF binders measured at a C/2 rate (2100 mA g^{-1}). Si NPs: Super P: binder = 60:20:20 by weight. c) The cycling performance of the Si electrodes employing the PAA-C and PAA binders measured at C/2 rate (2100 mA g^{-1}). Si NPs/ Super P/ binder = 60:20:20 by weight. d) The cycling performance of the Si NPs/graphite composite electrodes measured at 1 C rate (800 mA g^{-1}). These composite electrodes were prepared under the conditions active material/ Super P/ binder = 60:20:20 by weight, active material = 60% Si NPs/ 40% graphite by weight. All of the data in this figure are based on the electrolyte containing 3 wt% FEC additive.

the hydroxyl groups on the silicon oxide surfaces and the carboxylic acid moieties of the binders.[11,12] By contrast, the catechol-conjugated binders of Alg-C and PAA-C are expected to employ the dual adhesion mechanisms of hydrogen bonding and catecholic interaction with the Si NP surfaces. Particularly, as proved by the adhesion tests at both single-molecule (Figure 1) and bulk (Figure 2) scales, the catecholic interaction is far stronger than the other binding mechanisms provided by existing binders. The substantially higher capacities for Si-Alg-C and Si-PAA-C reflect very clearly the importance of the adhesive functions of the binders, suggesting the mussel-inspired catecholic adhesion as a new design principle for binders for Si anodes. Electrochemical impedance spectroscopy (EIS) data as well as surface imaging by scanning electron microscopy (SEM) consistently supported the catecholic effect and are presented in Figures S7 and S8, respectively.

The long-term cycling performance (Figures 3b–d) of all cells was also examined. For this investigation, we not only evaluated the effects of catechol but also endeavored to optimize other cell components beyond binders for the electrode to function in more practical conditions. We first assessed the effect of catechol on the cycle life of electrodes consisting of Si NPs alone with mass loadings of 0.2–0.3 mg cm^{-2} (Figures 3b,c) when cycled at C/2 rate. A well-known electrolyte additive, fluoroethylene carbonate (FEC),[41,42] was employed to improve the electrode/electrolyte interface and thus the cycle life. Data obtained in the absence of the additive are also presented in the Supporting Information (Figure S9) and are discussed below. From Figures 3b,c, the following points are noteworthy:

1) Consistent with the aforementioned adhesion tests, both Si-Alg-C and Si-Alg exhibit superior cycling performance compared to Si-PVDF (Figure 3b), indicating that the binding based on catecholic adhesion and hydrogen bonding is more effective for cycling performance than simple van der Waals interactions. After 400 cycles, both Si-Alg-C and Si-Alg fully retain their initial capacities, whereas the capacity of Si-PVDF drops very rapidly even at a low number of cycles and retains only 60% of its initial capacity after just 50 cycles. The Coulombic efficiencies after the precycling are, on average, 99.1% for Si-Alg-C and 99.2% for Si-Alg. In addition, Si-Alg-C also shows good rate capability (Supporting Information, Figure S10).

2) The Si-Alg-C and Si-Alg cells show similar capacity retention behaviors during cycling. However, commensurate with the precycling data, Si-Alg-C exhibits ~600 mAh g^{-1} larger capacities over the entire cycling range. Again, the increased capacities of Si-Alg-C are attributed to the enhanced adhesion by the catecholic interactions, which allows a larger proportion of Si NPs to participate in the alloying and de-alloying reactions with Li ions.[10] From this observation, it is anticipated that while catechol functional groups contribute to the capacity increase, the overall trend of capacity retention during cycling is affected mainly by the binder backbone. Similar results were observed for the cases of PAA and PAA-C binders as will be discussed in point 4) below.

3) The unusual capacity increases shown in Si-Alg and Si-Alg-C up to ~150 cycles are consistent results observed over multiple experiments (n = 5), confirming that the results are not caused by technical artifacts. Underlying mechanisms remain to be solved,[43,44] but current speculation is a synergistic effect of the binder backbone and the electrolyte additive. Cells utilizing the PAA binder (Figure 3c) or in the absence of the additive (Supporting Information, Figure S9) do not show such trends. A similar behavior in capacity increase was previously observed for the case where solid electrolyte interface (SEI) layers are stabilized by anisotropic volume expansion of Si[43] or the use of an additive,[44] which seemingly implies that the interfaces of Si-Alg-C and Si-Alg become stabilized by the addition of FEC.

4) Conjugation of catechol onto polymeric binder backbone might be a general method to increase the capacity of Si anodes. Similar results of capacity increase (Alg-C > Alg) were also observed for PAA binders (Figure 3c). Si-PAA-C shows a capacity increase (~220 mAh g^{-1}) over the entire cycle range compared to that of Si-PAA. This observation indicates that a number of other polymeric binders not tested in this study are candidates for catechol conjugation toward high capacity anode fabrication.

5) As shown in Figure S9 (Supporting Information), the same cells operated without FEC additive exhibit inferior cycling performance, indicating that the catechol groups and the additive play distinct roles in increasing capacity and improving cycle life, respectively.

Furthermore, the catechol-conjugated binders are demonstrated to be important players in practical anode settings. We extended our tests to a Si/graphite composite electrode (denoted as Si/Gr) in which approximately ten times the amount of active material was loaded (~2 mg cm^{-2}). In this particular case, Si and graphite constitute 60 and 40 wt%, respectively, of the active material. As mentioned above, obtaining an extended cycle life for Si NP electrodes has been a challenging task compared to other Si nanostructures, and increased mass loadings in Si NP electrodes showed unavoidable rapid capacity fading with increasing number of cycles.[45,46] As displayed in Figure 3d, over the whole range of 150 cycles, Si/Gr-Alg-C shows ~290 mAh g^{-1} higher capacities than Si/Gr-Alg, which is due to enhanced adhesion based on the catechol-mediated interactions and is also consistent with the results of the cases of Si NP alone. In addition to the catechol contribution to the increase of the cell's overall energy density, Si/Gr-Alg-C exhibits superior cycling performance compared to Si/Gr-Alg. After 150 cycles measured at 1 C, Si/Gr-Alg-C preserves 84.5% of the original capacity (805.8 mAh g^{-1}), whereas Si/Gr-Alg preserves only 62.8% of the original capacity (522.6 mAh g^{-1}) after the same number of cycles (Figure 3d). This capacity retention capability of Si/Gr-Alg-C is quite remarkable considering the situation of an order of magnitude increase in mass loading as well as its significant portion of Si NPs. The good cycling performance based on the Alg binder was recently reported for Si NP electrodes.[11] However, as indicated by the aforementioned data, the catecholic interactions turn out to be critical for good cycle lives of electrodes with increased mass loadings.

This investigation suggests that the binder plays a critical role in the operation of pure Si and Si-graphite composite anodes, and that mussel-inspired binders with extraordinary

wetness-resistant adhesion capability can contribute significantly to improving the capacities and cycle lives of Si NP-based anodes while remaining electrochemically stable at the given potentials. Moreover, this mussel-inspired binder should be readily applicable to other LIB electrodes that undergo significant volume change during cycling because the wetness-resistant catecholic adhesion proved to be effective with various substrates.[20]

Supporting Information

Supporting Information is available from the Wiley Online Library or from the author.

Acknowledgements

[1] M. S. Whittingham, *Chem. Rev.* **2004**, *104*, 4271.

[2] M. Armand, J. M. Tarascon, *Nature* **2008**, *451*, 652.

[3] J. M. Tarascon, M. Armand, *Nature* **2001**, *414*, 359.

[4] M.-H. Ryou, D. J. Lee, J. N. Lee, Y. M. Lee, J.-K. Park, J. W. Choi, *Adv. Energy Mater.* **2012**, *2*, 610.

[5] M.-H. Ryou, Y. M. Lee, J.-K. Park, J. W. Choi, *Adv. Mater.* **2011**, *23*, 3066.

[6] C. K. Chan, H. L. Peng, G. Liu, K. McIlwrath, X. F. Zhang, R. A. Huggins, Y. Cui, *Nat. Nanotechnol.* **2008**, *3*, 31.

[7] H. Kim, M. Seo, M. H. Park, J. Cho, *Angew. Chem. Int. Ed.* **2010**, *49*, 2146.

[8] T. Song, J. L. Xia, J. H. Lee, D. H. Lee, M. S. Kwon, J. M. Choi, J. Wu, S. K. Doo, H. Chang, W. I. Park, D. S. Zang, H. Kim, Y. G. Huang, K. C. Hwang, J. A. Rogers, U. Paik, *Nano Lett.* **2010**, *10*, 1710.

[9] T. H. Hwang, Y. M. Lee, B. S. Kong, J. S. Seo, J. W. Choi, *Nano Lett.* **2012**, *12*, 802.

[10] Z. Chen, L. Christensen, J. Dahn, *Electrochem. Commun.* **2003**, *5*, 919.

[11] I. Kovalenko, B. Zdyrko, A. Magasinski, B. Hertzberg, Z. Milicev, R. Burtovyy, I. Luzinov, G. Yushin, *Science* **2011**, *334*, 75.

[12] A. Magasinski, B. Zdyrko, I. Kovalenko, B. Hertzberg, R. Burtovyy, C. F. Huebner, T. F. Fuller, I. Luzinov, G. Yushin, *ACS Appl. Mater. Interfaces* **2010**, *2*, 3004.

[13] P. Vukusic, J. R. Sambles, *Nature* **2003**, *424*, 852.

[14] F. Xia, L. Jiang, *Adv. Mater.* **2008**, *20*, 2842.

[15] K. Autumn, M. Sitti, Y. C. A. Liang, A. M. Peattie, W. R. Hansen, S. Sponberg, T. W. Kenny, R. Fearing, J. N. Israelachvili, R. J. Full, *Proc. Natl. Acad. Sci. USA* **2002**, *99*, 12252.

[16] H. Lee, B. P. Lee, P. B. Messersmith, *Nature* **2007**, *448*, 338.

[17] J. H. Waite, M. L. Tanzer, *Science* **1981**, *212*, 1038.

[18] Q. Lin, D. Gourdon, C. J. Sun, N. Holten-Andersen, T. H. Anderson, J. H. Waite, J. N. Israelachvili, *Proc. Natl. Acad. Sci. USA* **2007**, *104*, 3782.

[19] S. M. Kang, M.-H. Ryou, J. W. Choi, H. Lee, *Chem. Mater.* **2012**, *24*, 3481.

[20] H. Lee, S. M. Dellatore, W. M. Miller, P. B. Messersmith, *Science* **2007**, *318*, 426.

[21] H. Lee, N. F. Scherer, P. B. Messersmith, *Proc. Natl. Acad. Sci. USA* **2006**, *103*, 12999.

[22] C. R. Matos-Perez, J. D. White, J. J. Wilker, *J. Am. Chem. Soc.* **2012**, *134*, 9498.

[23] N. S. Choi, K. H. Yew, W. U. Choi, S. S. Kim, *J. Power Sources* **2008**, *177*, 590.

[24] N. Hochgatterer, M. Schweiger, S. Koller, P. Raimann, T. Wöhrle, C. Wurm, M. Winter, *Electrochem. Solid-State Lett.* **2008**, *11*, A76.

[25] H. Buqa, M. Holzapfel, F. Krumeich, C. Veit, P. Novak, *J. Power Sources* **2006**, *161*, 617.

[26] S. Komaba, N. Shimomura, N. Yabuuchi, T. Ozeki, K. Yui, K. Konno, *J. Phys. Chem. C* **2011**, *115*, 13487.

[27] N. Yabuuchi, K. Shimomura, Y. Shimbe, T. Ozeki, J. Y. Son, H. Oji, Y. Katayama, T. Miura, S. Komaba, *Adv. Energy Mater.* **2011**, *1*, 759.

[28] J. A. Rowley, G. Madlambayan, D. J. Mooney, *Biomaterials* **1999**, *20*, 45.

[29] I. You, S. M. Kang, Y. Byun, H. Lee, *Bioconjug. Chem.* **2011**, *22*, 1264.

[30] F. Kienberger, G. Kada, H. J. Gruber, V. P. Pastushenko, C. Riener, M. Trieb, H. G. Knaus, H. Schindler, P. Hinterdorfer, *Single Mol.* **2000**, *1*, 59.

[31] M. Rief, H. Clausen-Schaumann, H. E. Gaub, *Nat. Struct. Mol. Biol.* **1999**, *6*, 346.

[32] W. R. Liu, M. H. Yang, H. C. Wu, S. M. Chiao, N. L. Wu, *Electrochem. Solid-State Lett.* **2005**, *8*, A100.

[33] Y. H. Xu, G. P. Yin, Y. L. Ma, P. J. Zuo, X. Q. Cheng, *J. Power Sources* **2010**, *195*, 2069.

[34] M. Yu, J. Hwang, T. J. Deming, *J. Am. Chem. Soc.* **1999**, *121*, 5825.

[35] M. Mehdizadeh, H. Weng, D. Gyawali, L. Tang, J. Yang, *Biomaterials* **2012**, *33*, 7972.

[36] H. O. Ham, Z. Liu, K. Lau, H. Lee, P. B. Messersmith, *Angew. Chem. Int. Ed.* **2011**, *50*, 732.

[37] J. Guo, X. Chen, C. Wang, *J. Mater. Chem.* **2010**, *20*, 5035.

[38] L. B. Chen, X. H. Xie, J. Y. Xie, K. Wang, J. Yang, *J. Appl. Electrochem.* **2006**, *36*, 1099.

[39] L. Zheng, L. Xiong, D. Zheng, Y. Li, Q. Liu, K. Han, W. Liu, K. Tao, S. Yang, J. Xia, *Talanta* **2011**, *85*, 43.

[40] A. Kiani, J. B. Raoof, D. Nematollahi, R. Ojani, *Electroanalysis* **2005**, *17*, 1755.

[41] M.-H. Ryou, G. B. Han, Y. M. Lee, J. N. Lee, D. J. Lee, Y. O. Yoon, J.-K. Park, *Electrochim. Acta* **2010**, *55*, 2073.

[42] N. S. Choi, K. H. Yew, K. Y. Lee, M. Sung, H. Kim, S. S. Kim, *J. Power Sources* **2006**, *161*, 1254.

[43] H. Wu, G. Chan, J. W. Choi, I. Ryu, Y. Yao, M. T. McDowell, S. W. Lee, A. Jackson, Y. Yang, L. Hu, *Nat. Nanotechnol.* **2012**, *7*, 310.

[44] Y. M. Lin, K. C. Klavetter, P. R. Abel, N. C. Davy, J. L. Snider, A. Heller, C. Mullins, *Chem. Commun.* **2012**, *48*, 7268.

[45] M. Yoshio, T. Tsumura, N. Dimov, *J. Power Sources* **2005**, *146*, 10.

[46] Y. Oumellal, N. Delpuech, D. Mazouzi, N. Dupré, J. Gaubicher, P. Moreau, P. Soudan, B. Lestriez, D. Guyomard, *J. Mater. Chem.* **2011**, *21*, 6201.